Structure Development and Interfacial Interactions in High-Density Polyethylene/Hydroxyapatite (HDPE/HA) Composites Molded with Preferred Orientation

Rui A. Sousa,[1,2]* Rui L. Reis, António M. Cunha,[1] Michael J. Bevis[2]

[1]*Department of Polymer Engineering, University of Minho, 4800-058 Guimarães, Portugal*
[2]*Wolfson Centre for Materials Processing, Brunel University, Uxbridge, Middlesex, UB8 3PH, United Kingdom*

Received 24 January 2002; revised 22 March 2002; accepted

ABSTRACT: Composites of high-density polyethylene (HDPE) filled with sintered and nonsintered hydroxyapatite (HA) powders, designated as HAs and HAns, respectively, were compounded by twin screw extrusion. Compounds with neoalkoxy titanate or zirconate coupling agents were also produced to improve interfacial interaction and filler dispersion in the composites. The composites were molded into tensile test bars using (i) conventional injection molding and (ii) shear-controlled orientation in injection molding (SCORIM). This latter molding technique was used to deliberately induce a strong anisotropic character to the composites. The mechanical characterization included tensile testing and microhardness measurements. The morphology of the moldings was studied by both polarized light microscopy and scanning electron microscopy, and the structure developed was assessed by wide-angle X-ray diffraction. The reinforcing effect of HA particles was found to depend on the molding technique employed. The higher mechanical performance of SCORIM processed composites results from the much higher orientation of the matrix and, to a lesser extent, from the superior degree of filler dispersion compared with conventional moldings. The strong anisotropy of the SCORIM moldings is associated with a clear laminated morphology developed during shear application stage. The titanate and the zirconate coupling agents caused significant variations in the tensile test behavior, but their influence was strongly dependent on the molding technique employed. The application of shear associated with the use of coupling agents promotes the disruption of the HA agglomerates and improves mechanical performance. J Appl Polym Sci 86: 2873–2886, 2002

Key words: high-density polyethylene (HDPE); hydroxyapatite; composites; biomaterials; injection molding; injection molding; shear-controlled orientation in injection molding (SCORIM)

INTRODUCTION

In an engineering perspective, bone can be considered as a complex composite material, comprised of a polymer matrix (collagen fibrils) and an inorganic stiff phase [hydroxyapatite crystals (HA)].[1–3] The combination of low density and high mechanical performance (featuring high stiffness and strength, strong anisotropy, and pronounced viscoelastic behavior) arises from its composition and structure, as well as from the arrangement of the bone constituent elements at different scale levels.[3–9] As a result, the mechanical behavior of human bone varies considerably with its morphology, depending on a large range of features, such as the type, its location, and the personal characteristics of the patient.[10–12] Nevertheless, it is possible to characterize bone with values of tensile modulus, in the longitudinal direction, in the range 7–25 GPa.[10–12]

When developing bone substitute materials, the mechanical behavior is a crucial aspect because the stiffness of the implant determines the amount of load carried by the healing/surrounding tissue.[13,14] It is known that bone remodeling strongly depends on an adequate loading of the healing bone that strictly relies on the stiffness of the implant.[13,14] Thus, the replacement of hard tissues in load-bearing applications demands mechanically biocompatible materials with properties similar to those of the bone.

Polymer-based composites are a class of materials that may, in principle, combine adequately high stiffness and strength together with a clear anisotropic and viscoelastic character. Bonfield et al.[15–32] introduced the bone-analogue concept by proposing composites composed of a ductile polymer matrix [polyethylene (PE)] and a stiff ceramic phase (HA). The idea was to mimic bone by using a semicrystalline matrix that can develop a considerable anisotropic character through adequate orientation techniques reinforced with a bone-like ceramic that also assures the mechanical reinforcement and the bioactive character of the composite.[17,18,24] Attempts to develop a bone-matching mechanical performance have relied on the use of

Correspondence to: R. A. Sousa (rui.sousa@set.pt).
*Current address: IBEROMOLDES, S.A., Rua Augusto Costa, Picassinos P.O. Box 33, 2431-956 Marinha Grande, Portugal

hydrostatic extrusion,[24–26] PE fiber reinforcement,[27,28] and chemical coupling.[29–32] The application of hydrostatic extrusion to process high density PE (HDPE)/HA composites has been shown to be a successful route for the production of composites with high anisotropic character and improved mechanical performance.[24] However, the respective geometry and dimensions were constrained by the limitations of an extrusion-based technique, which inhibits the production of very thick or geometrically complex parts. Further improvements of stiffness have been achieved through (i) the combined use of hydrostatic extrusion with short PE fiber reinforcement,[27] or (ii) the woven PE fiber reinforcement of the HDPE/HA matrix.[28] In both cases, the use of very stiff and chemically compatible fiber enabled the attainment of values of stiffness and strength in the bounds of human cortical bone[24] or within its typical range of mechanical performance.[27,28] Parallel investigations[29–32] concerning the chemical coupling of PE/HA composites were based on the use of silane agents and acrylic acid grafting on PE. Such methodology allowed for the enhancement of tensile strength and ductility, but did not result in consistent improvements of stiffness for different HA volume contents, which was attributed to a plasticizer effect of the silane agent for high HA contents.[29]

An alternative approach to the mechanical performance enhancement of HDPE/HA composites was followed by Reis et al.[33] with the use of shear-controlled orientation injection molding (SCORIM). The SCORIM operation is based on the application of a macroscopic shear stress field at the melt/solid interface of the polymer during the molding cycle. This molding technique proved to be a successful approach for the inducement of an anisotropic character in HDPE[34] and in the respective composites with HA.[33] X-ray diffraction (XRD) patterns and calorimetric studies on SCORIM-processed HDPE have revealed, respectively, signs of C-axis orientation parallel to flow direction and high levels of crystallinity, which were not observed in conventionally molded specimens.[34] As a result, values of 7.4 GPa and 74 MPa (in the bounds of human cortical bone) have been achieved for the tensile modulus and the tensile strength of HDPE/HA composites, respectively. In spite of the ability of SCORIM to control, to a certain extent, the structure development of the HDPE matrix and, as a result, induce a clear anisotropic mechanical behavior into the molded part, the performance of the HDPE/HA composites is still below the envisaged goal. This lack of performance is mostly attributable to the HA particles, which are efficient from a bioactivity point of view, but inefficient as a mechanical reinforcement of the polymeric matrix. The poor stiffening effect of HA powders results from both their particulate nature (low aspect ratio) and the very distinct chemical characters of the HDPE and HA phases. These two aspects limit the load transfer in the composite and restrict the final mechanical behavior. So, the enhancement in mechanical performance of these systems will depend on the successful combination of an adequate structure development control with an enhancement in the filler/matrix interaction.

The interaction between a polymer matrix and a filler can be (i) mechanical, when it results from the radial compression forces exerted by the polymer on the filler particles developed during cooling due to thermal contraction, or (ii) of predominant chemical nature, when the reactivity of the filler towards the matrix has an important role. In the latter case, it is important to distinguish physical interaction from chemical bonding. According to Wypych,[35] physical interaction is more or less temporary, implicating hydrogen bonding or van der Waals forces, whereas chemical bonding is stronger and more permanent, involving covalent bond formation. Both modes of interaction involve chemical bonds that can be disrupted with dissimilar energy inputs. If the primary effect of a processing additive is to increase the interaction between the polymer and the matrix, such an additive can be regarded as a coupling agent.[36] Coupling agents establish chemical bridges between the matrix and the filler, promoting the adhesion between the phases. In many cases, their effect is not unique, influencing also the rheology of the compound. Organotitanates and organozirconates are two surface modifiers with analogous structures and functioning principles that can be used for filler modification. The latter may be preferable in certain applications because of the high instability of the titanate agent.[37] Several studies[38–49] contain examples of the application of titanate[38–47] or zirconate[48,49] surface modifiers, alone or in combination with other coupling agents, to a wide range of composite systems.

The structure development and interfacial interactions in injection molding of HDPE/HA composites are compared in this paper. SCORIM was used to develop a high degree of orientation in the molded part and mimic the bone mechanical anisotropy. The effect of titanate and zirconate coupling agents, aimed to improve the interfacial interaction between the filler and the matrix, in the mechanical performance of the composites is also described. The mechanical performance of the molded composites is explained in terms of the thermomechanical environment during processing and correlated with the respective structure development of the matrix.

EXPERIMENTAL

Materials

The studied material was a high-density polyethylene (HDPE), grade GM 9255 F, supplied by Elenac GmbH

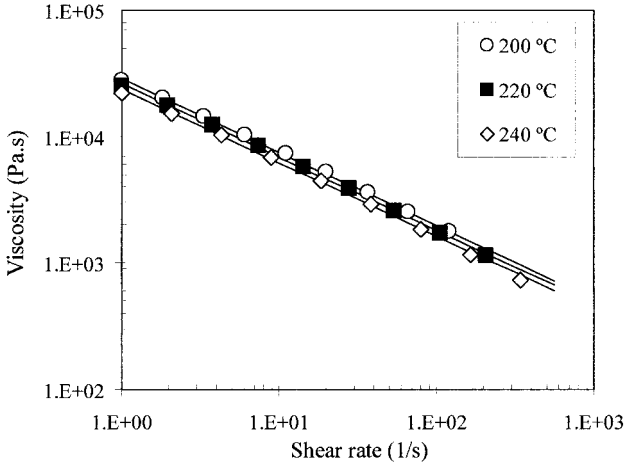

Figure 1 Flow curves for HDPE GM9255 F.

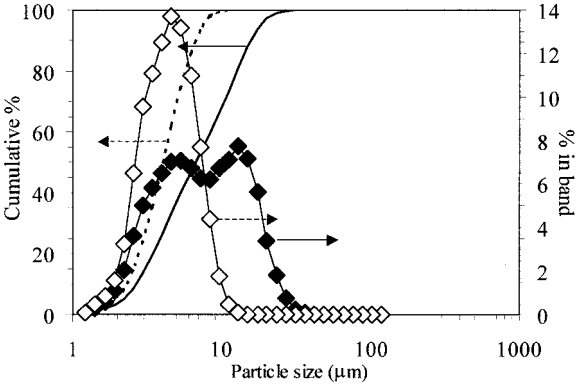

Figure 2 Particle size distributions for (♦) the sintered (HAs) and (◇) the non-sintered (HAns) hydroxyapatite powders.

(Germany), with melt flow rates (MFR) of 0.28 g/10 min (190 °C, kg) and 9.50 g/10 min (190 °C, 21.6 kg). This HDPE is a typical blow molding grade, with a molecular weight distribution characterized by a high molecular weight tail.[50] The respective flow curves are presented in Figure 1. The general properties as quoted by the respective producer are shown in Table I.

Composites of HDPE with hydroxyapatite (HA) were produced using two commercially available synthetic HA grades: (i) a sintered HA (HAs) and (ii) a nonsintered HA (HAns), both supplied by Plasma Biotal Ltd. (United Kingdom) under the trade name Captal. The two powders differ physically in terms of the granulometric dispersion and specific surface area. The respective granulometric distributions are presented in Figure 2. HAs exhibits sample and secondary modes at 12.9 and 5.3 μm, respectively, and an average particle size of 10.1 μm. HAns presents a unimodal distribution with a sample mode at 4.6 μm and an average particle size of 5.9 μm. The surface areas of HAs are 0.38 m^2/g (1.19 m^2/cm^3), and those of HAns are 0.56 m^2/g (1.73 m^2/cm^3). Processing optimization studies were conducted with a compound of HDPE with calcium apatite obtained by calcination of bone ashes (further referred as BA). BA powder presents a unimodal particle size distribution with an average particle size of 28.14 μm and a sample mode of 45.75 μm.

Coupled HDPE/HA composites were produced using two neoalkoxy coupling agents: (i) a neopentyl-(dially)oxytri(dioctyl)phosphato titanate (LICA 12), and (ii) a neopentyl(dially)oxy, tri(dioctyl)phosphato zirconate (NZ 12) supplied by Kenrich Petrochemicals (). The chemical structure and physical properties of these agents are presented in Table II.

TABLE I
Properties of HDPE GM 9255 F[a]

Density (g/cm^3)	Modulus (GPa)	Stress at Yield (MPa)
0.955	1.15	27

[a] From ref. 35.

Twin screw extrusion (TSE)

Composites of HDPE with 25 wt % (by weight) HAs or HAns powders were produced in a Leistritz AG-LSM 36/25D modular co-rotating twin-screw extruder. A temperature profile of 160/165/170/175/180/185/190/180 °C and a screw speed of 100 rpm were used during compounding. The average output rates were 2.94 and 2.83 kg/h for the HDPE/HAs and the HDPE/HAns composites, respectively. The cooling of the extrudate was performed in air with an average temperature of 17 °C.

Coupled composites, based on the titanate and the zirconate agents, were also produced for both fillers under the aforementioned conditions. For all cases, the coupling agent weight percentage was defined relatively to the amount of the filler and added directly to the polymer and filler mixture before extrusion. The reactivity of these coupling agents towards the surface-active species before it is combined with the polymer and the filler is high, which may cause their premature side reaction.[51] To minimize the side reaction of these agents with available functional groups inside the extruder, a preliminary extrusion of a compound of HDPE with 0.5 wt % of the coupling agent was performed. The objective of this procedure was to promote the primary reaction of the neoalkoxy agents with available functional groups at both the surface of the screw and the barrel, minimizing, as much as possible, the surface condensation of the additive during the compounding stage.

The formulations produced with the titanate and the zirconate additives are summarized in Table III. The coupling agent dosage in the composite varied proportionally to the respective surface area of the HA

TABLE II
Chemical Structure and Physical Properties of Neoalkoxy Coupling Agents[a]

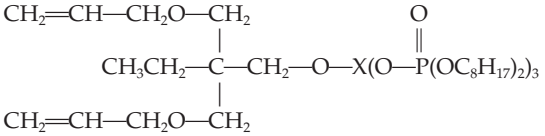

	ρ (g/cm^3)	η^b (cPs)	pH
Neoalkoxy titanate (X = Ti) − LICA 12	1.03	1800	5.5
Neoalkoxy zirconate (X = Zr) − NZ 12	1.06	160	6.0

[a] From ref. [51]. [b] At 25 °C.

powder employed: 0.25–0.75 wt % for the HAs (0.38 m^2/g) and 0.50–1.00 wt % for the HAns (0.56 m^2/g).

All the extrudates were pelletized after cooling, for the subsequent use in the injection molding stage, with a rotating knife.

Injection molding

The composites produced were molded into axisymmetric tensile test bars with 5-mm cross-section diameter and 25-mm gauge length (see schematic representation in Figure 3). The specimens were molded in a Demag D-150 NCIII-K injection molding machine fitted with a SCORIM device. As shown in Figure 3, the conventional molding geometry presents a single gate system, whereas the SCORIM geometry presents a double gate system.

During the solidification stage of a typical SCORIM cycle, the melt is continuously displaced inside the mold, which causes the application of a macroscopic shear stress field at the melt/solid interface. This process is assured by the operation of two hydraulically actuated pistons that displace the melt inside the mold during the holding pressure stage. These pistons can actuate according to three possible modes of operation: A, B, and C. In mode A, both pistons actuate out-of-phase, causing the melt inside the mold to be continuously sheared. Conversely, in mode B, both pistons actuate in-phase, which causes the successive compression and decompression of the molten material inside the mold. Finally, in mode C, both pistons are held down together, causing the packing of the material inside the mold. These operation modes can be combined sequentially in several stages during injection molding, enabling an almost infinite number of processing programmes.

TABLE III
Formulations Developed for the HDPE/HA Composites

	Coupling Agent Weight Amount (%)[a]	
Composite	LICA 12	NZ 12
25 wt % HAns	0.50, 1.00	0.50, 1.00
25 wt % HAs	0.25, 0.50, 0.75	0.25, 0.50, 0.75

[a] Relative to the filler amount.

The SCORIM setup conditions were optimized with HDPE/BA composites, following a design of experiments (DOE) plan. In this stage, four processing parameters were studied; namely, the holding pressure, the piston pressures (packing and relaxation), the frequency of piston movements, and the duration of applied shear. The combination of these processing parameters was made according to a L8 (2^{4-1}) orthogonal array. The central point of this experimental array corresponded to the SCORIM operating conditions that maximized the mechanical properties (following a maximum stiffness criteria) of an unreinforced HDPE grade.[34] The best combination of processing conditions within this array was then used to process the HDPE/HA composites. The processing conditions for CM and SCORIM moldings are presented in Table IV. The SCORIM cycle consisted of the application of a single stage using Mode A operation. The typical cavity pressure profile during conventional molding and SCORIM processing of HDPE/HA composites is shown in Figure 4. The oscillating cavity pressure evolution for SCORIM processed moldings results from the alternate actuation of the pistons.

Tensile testing

The tensile tests were performed to assess the mechanical performance of the moldings on an Instron 4505 universal testing machine, using an Instron 2630 resis-

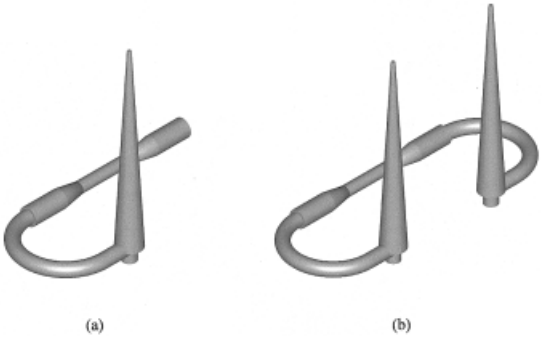

Figure 3 Schematic diagram of the moldings (including runner system) produced by (a) conventional molding and (b) SCORIM.

tive extensometer with 10-mm gauge length. The tensile bars were tested to determine the tangent modulus (E_t), the ultimate tensile strength (UTS), and the strain at break (ϵ_b). These tests were performed in a controlled environment (23 °C and 55% RH). The cross-head speed was 5 mm/min. (8.3×10^{-5} m/s) until 1.5 % strain, to accurately determine the modulus, and then increased to 50 mm/min. (8.3×10^{-4} m/s).

The significance between the means of different sets was evaluated by t tests. A confidence level of 99% was used for all the tests, except when stated otherwise.

Microhardness

The variation in mechanical performance along the part diameter was investigated by microhardness measurements. The experiments were carried out at room temperature in selected specimens, along the cross-section diameter, in a Leica VMHT30A equipped with a Vickers diamond indenter, using a load of 2.94 N and a dwell time of 5 s. The values of hardness were obtained with the following equation

$$H = 1.854 \frac{P}{d^2} \quad (1)$$

where P is the load and d is the length of the indentation.

Polarized light microscopy (PLM)

The resistant length of the tensile test bars were removed and mounted in an epoxy resin. A microtome was used to cut slices of the cross section with an average thickness of 15 μm from the middle region of the gauge length. The slices obtained were observed by optical polarized light microscopy (PLM) in an Olympus BH-A microscope.

TABLE IV
Processing Conditions for Conventional and SCORIM Moldings of HDPE-Based Composites

Processing Condition	Conventional	SCORIM
Injection pressure (MPa)[a]	13.8	13.8
Holding pressure (MPa)[a]	8.8	7.6
Injection time (s)	0.5	0.5
Holding pressure time (s)	15.0	30.0
Cooling time (s)	15.0	15.0
Cycle time (s)		
Mold temperature (°C)	40	40
Melt temperature (°C)	190	190
Number of SCORIM stages	—	1
Stage duration (s)	—	30
Frequency of piston movements (Hz)	—	1.0
Piston pressures (%)	—	50

[a] Pressures in the hydraulic system of the machine.

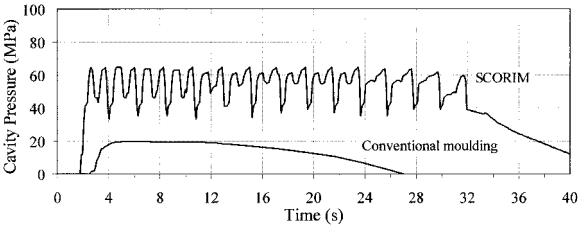

Figure 4 Typical cavity pressure profile for during conventional molding and SCORIM processing of HDPE/HA composites.

Scanning electron microscopy (SEM)

Scanning electron microscopy (SEM) was performed for fractographic analysis. Microscopy was performed on selected sets on a Leica Cambridge scanning electron microscope. All the surfaces were mounted on a copper stub and coated with Au/Pd alloy prior to examination.

Wide-angle X-ray diffraction (WAXD) and X-ray Patterns

The microstructure of the moldings was also investigated by X-ray diffraction and patterns. Ni filtered Cu Kα radiation with a wavelength of 0.1517 nm at 36 kV and 26 mA was used to obtain WAXD spectra in a Philips 1050 diffractometer. The diffraction data was acquired at a rate of 0.02° 2θ/s and over a Bragg angle range of $5° < 2\theta < 50°$ for samples with 1-mm thickness.

The X-ray patterns were recorded for selected samples to assess the preferred orientation of the crystalline phase. Specimens were taken from the central area of the gauge length and mounted in a Philips microcamera. The X-ray beam was oriented parallel to the thickness of the sample and perpendicular to the flow direction. An aperture of 100 μm of diameter was used to define the position and cross section of the incident X-ray beam. Debye patterns were obtained for the moldings at positions of 0.1, 0.5, 1.0, and 4.0 mm from the edge of the moldings.

RESULTS AND DISCUSSION

Mechanical performance of HDPE/HA composites

The variation of tangent modulus (E_t) for conventionally injection molded and SCORIM processed HDPE/HAs composites as a function of the amount of titanate or zirconate coupling agents is shown in Figure 5. In Figures 5 to 10, the straight dashed line represents the respective mechanical property of unreinforced

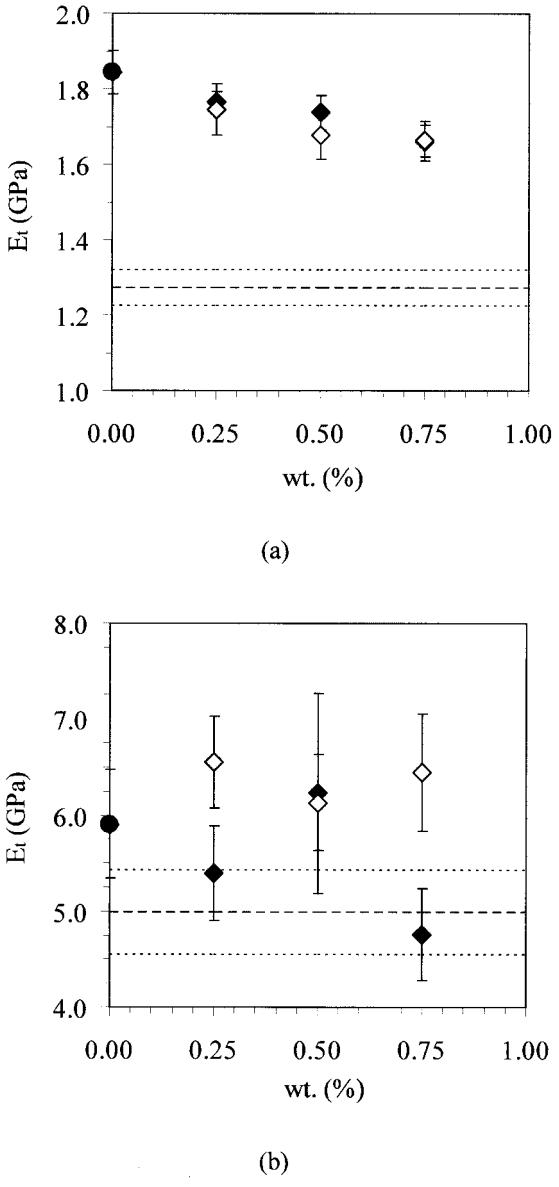

Figure 5 Variation of E_t for (a) conventionally injection molded and (b) SCORIM-processed HDPE/HAs composites as a function of the (♦) titanate or (◇) zirconate coupling agent content together with the reference E_t for the unreinforced HDPE (- - -) ± the respective standard deviation (· · ·).

HDPE processed under identical conditions, whereas the dotted straight lines represent the respective standard deviation limits of such property. The black circle plotted for 0 wt % indicates the mechanical property value for the HDPE/HA composite without any coupling agent.

The results in Figure 5 indicate that the relative stiffness improvement obtained as a result of HA reinforcement differs for both molding techniques. In conventional molding (Figure 5a), the incorporation of HA particles in HDPE leads to an improvement in E_t of 45% (from 1.3 to 1.8 GPa), whereas in SCORIM (Figure 5b), it leads to a 18% improvement (from 5.0 to 5.9 GPa). The values of stiffness for conventionally injection molded HDPE/HAs composites are in the range encountered for a similar system processed by the same method.[52] The application of SCORIM to the processing of HDPE and HDPE/HAs composites results in improvements in stiffness of 290 and 225%, respectively, compared with conventional molding. The decrease in the matrix volume content, as a result of HA incorporation, reduces the magnitude of the shear application effect in the stiffness of the molded part. In spite of this effect, the inclusion of HA particles in SCORIM-processed specimens leads to an absolute increase in stiffness of 0.9 GPa, which is higher than the increase of 0.5 GPa obtained for conventional molding. The reinforcement effect of the HA particles seems to be enhanced by the application of shear. The use of titanate or zirconate additives, in conventional molding (Figure 5a), leads in both cases to a decrease in the measured stiffness (that is proportional to the coupling agent weight content), indicating a plasticizer effect of these additives. This effect is not observed for SCORIM-processed specimens (Figure 5b), where the two coupling agents cause distinct results. Concerning the titanate agent, no significant variation in stiffness is observed for 0.25 and 0.50 wt %. For 0.75 wt %, a decrease in E_t occurs (significant at 95% confidence level). On the contrary, the zirconate agent has a positive effect on the E_t (from 5.9 to 6.5 GPa) of the HDPE/HAs composites (statistically significant at 90% confidence level) for a weight content of 0.25%. For higher weight contents, this agent does not influence the measured stiffness.

The variation in the ultimate tensile strength (UTS) for the HDPE/HAs composites is plotted in Figure 6 for both conventional molding (Figure 6a) and SCORIM (Figure 6b). The inclusion of HAs particles in HDPE results in reductions of UTS of 3 and 7% (significant at 95% confidence level) for conventional molding and SCORIM, respectively. For conventional molding, this decrease becomes more pronounced with the addition of the titanate or zirconate agents. This trend is not observed in the SCORIM-processed specimens. For 0.25 and 0.50 wt % of titanate, no significant variation in tensile strength is observed, whereas for 0.75 wt %, a 5.9% improvement (from 81 to 86 MPa) is achieved (significant at 95% confidence level).

For the case of zirconate, the strength of the composite is enhanced for all compositions, with increases of 11, 8, and 9% for weight contents of 0.25, 0.50, and 0.75% respectively. For 0.25 wt % zirconate, it is possible to produce HDPE/HAs moldings with higher stiffness than and equivalent tensile strength as unreinforced HDPE. This enhancement can be attributed to an increase in the particle dispersion, to an improvement in the filler/matrix interaction, or to both factors simultaneously. In spite of this enhancement, it is obvious from the results presented that the coupling

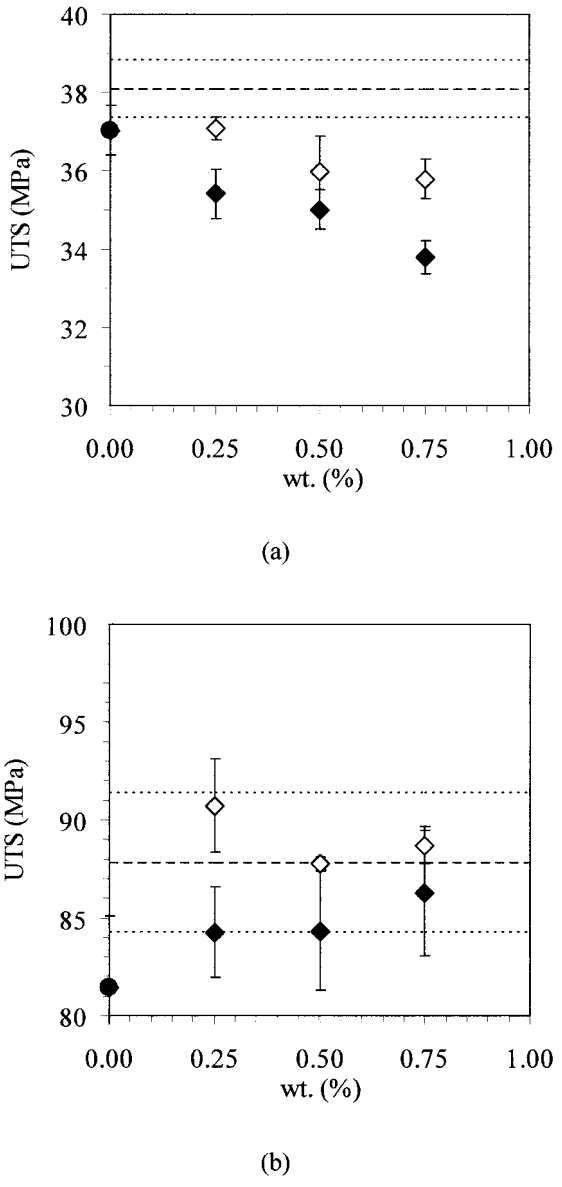

Figure 6 - Variation of UTS for (a) conventionally injection molded and (b) SCORIM-processed HDPE/HAs composites as a function of the (♦) titanate or (◇) zirconate coupling agent content together with the reference UTS for the unreinforced HDPE (- - -) ± the respective standard deviation (· · ·).

agent effect strongly depends on the processing route employed.

The variation of the strain at break (ϵ_b) for the conventionally injection molded and the SCORIM-processed HDPE/HAs composites as a function of the titanate or the zirconate weight contents is plotted in Figure 7. The reinforcement of HDPE with HA particles reduces the ductility on tensile testing of conventionally molded specimens by 54% (Figure 7a). This decrease is attenuated by the addition of any of the coupling agents studied. For the conventionally injection molded coupled composites, a maximum ϵ_b value of 34% is attained for 0.75 wt % of titanate. The decrease in ductility on HA reinforcement is not observed in the SCORIM-processed composites (Figure 7a). It is possible to produce HDPE/HAs composites with the same ductility as unreinforced HDPE (ϵ_b of 14%). The use of zirconate improves the ductility of the composites compared with the uncoupled HDPE/HAs formulation, allowing for a maximum improvement in ϵ_b of 53% for a weight amount of 0.50%. The influence of the coupling agent on the mechanical performance of the composite greatly depends on the thermomechanical history (i.e., processing route).

The variation of E_t for SCORIM-processed HDPE/HAns composites is plotted in Figure 8 as a function of

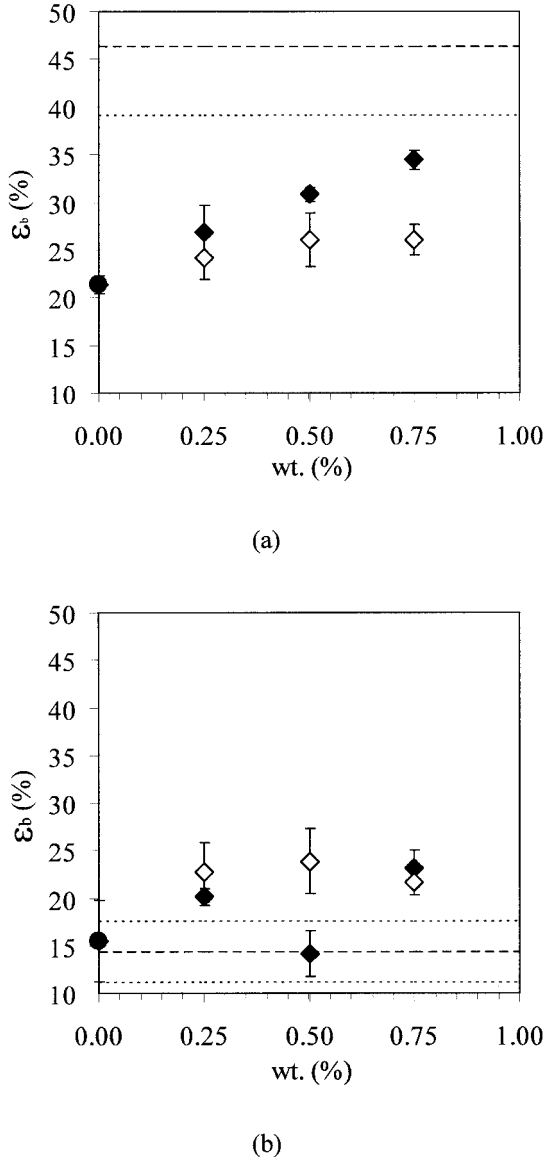

Figure 7 Variation of ϵ_b for (a) conventionally injection molded and (b) SCORIM-processed HDPE/HAs composites as a function of the (♦) titanate or (◇) zirconate coupling agent content together with the reference ϵ_b for the unreinforced HDPE (- - -) ± the respective standard deviation (· · ·).

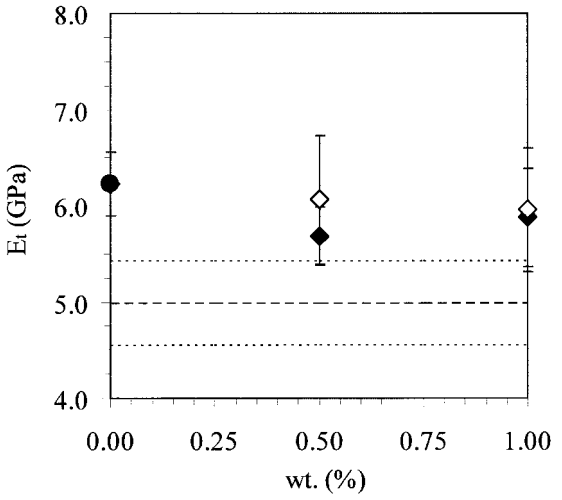

Figure 8 Variation of E_t for SCORIM-processed HDPE/HAns composites as a function of the (♦) titanate or (◇) zirconate coupling agent content together with the reference E_t for the unreinforced HDPE (- - -) ± the respective standard deviation (· · ·).

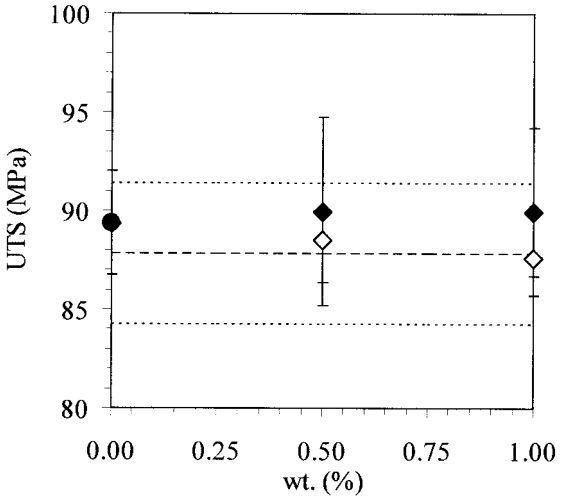

Figure 9 Variation of UTS for SCORIM-processed HDPE/HAns composites as a function of the (♦) titanate or (◇) zirconate coupling agent content together with the reference UTS for the unreinforced HDPE (- - -) ± the respective standard deviation (· · ·).

the weight amount of titanate or the zirconate agents (conventional molding was not employed for the HDPE/HAns composites). The reinforcement of HDPE with HAns particles improves the stiffness by 20%, from 5.0 to 6.2 GPa. The higher stiffness values obtained for the HAns particles with lower average size as compared with the HAs particles is in agreement with the results reported by Wang et al.[53] on the influence of HA particle size on the mechanical performance of HDPE/HA composites. However, this sort of dependence of stiffness on the particulate size is not always observed in particulate-filled composites, as shown by the study of Xavier et al.[54] on the study of mica-filled polypropylene composites, where coarser mica particles caused stiffer composites. The mechanical properties in particulate-filled composites are determined by small amounts of particles within a critical size range and not uniquely by the average particle size. For the coupled compositions, the only significant variation in stiffness was observed for 0.50 wt % of titanate for which a decrease in E_t from 6.2 to 5.7 GPa occurs (significant at 95% confidence level).

The variation of UTS for SCORIM-processed HDPE/HAns composites as a function of the titanate or the zirconate weight content is plotted in Figure 9. It is possible to enhance the stiffness of HDPE by HAns reinforcement without affecting its strength. HDPE/HAns composites present a UTS of 89 MPa, which is maintained on the addition of any of the coupling agents investigated.

The variation of ϵ_b for SCORIM-processed HDPE/HAns composites as a function of the titanate or the zirconate coupling agent amount is plotted in Figure 10. HDPE/HAns composites present an ϵ_b of 29.4%, which accounts for increases of 103 and 112% compared with HDPE and HDPE/HAs composites, respectively. The addition of the coupling agents does not affect the ductility of the composite. For SCORIM-processed composites, the presence of HA particles reduces the brittleness of HDPE. The higher ductility of the composites, especially for the HAns-reinforced composites compared with the unreinforced HDPE is, at a first glance, surprising because one of the purposes of the HA particles is to reinforce the ductile polymer matrix. The increase in ductility obtained with the HA reinforcement has been already observed for SCORIM-processed materials.[33] A similar effect was also observed for particulate-filled polypro-

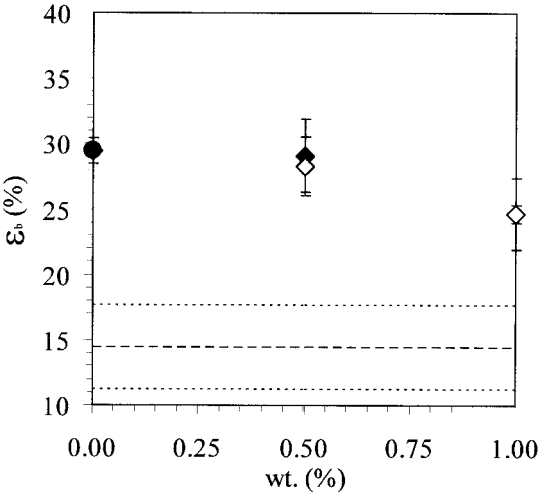

Figure 10 Variation of ϵ_b for SCORIM-processed HDPE/HAns composites as a function of the (♦) titanate or (◇) zirconate coupling agent content together with the reference ϵ_b for the unreinforced HDPE (- - -) ± the respective standard deviation (· · ·).

pylene,[54] where the enhancement of ductility with particulate loading was explained by the existence of a crack-pinning-controlled fracture propagation process. During plastic deformation, the crack initiated is temporarily pinned at the particle surface, allowing sufficient time to elapse for the occurrence of considerable localized plastic deformation.

Structure development of the HDPE Matrix

The SEM photographs of the tensile fracture surfaces on tensile testing of conventionally injection molded composites are plotted in Figures 11a and 11b, and those of SCORIM-processed HDPE/HAs composites are plotted in Figures 11c and 11d. The tensile fracture surface of conventional moldings exhibits two distinct zones: a relatively brittle outer layer in the vicinity of the mold wall and a more ductile core that assures most of the deformation during tensile testing. Conversely, SCORIM moldings present a clear laminated morphology developed during shear application, where it is possible to distinguish three well-defined zones: a skin layer, a core region, and a layered zone in between. Previous work[34] has shown that this peculiar morphology, developed as a result of the out-of-phase operation of the SCORIM pistons, is associated with flow-induced crystallized structures designated as shish-kebab. The enhancement of stiffness observed in PE exhibiting a shish-kebab structure arises from both the highly anisotropic character of the chain-extended crystallized fiber (shish) and the interlocking effect between adjacent platelets (kebab) that give rise to a zip-fastener morphology.[55–57] The development of these structures is very much dependent on the molecular weight and molecular weight distribution.[56,57] The high end of the molecular weight distribution contributes to the formation of the chain-extended fibrils. This fact, together with the higher chemical stability of high molecular weight polymers desirable for the intended field of application, justifies the use of the studied HDPE grade in the present work.

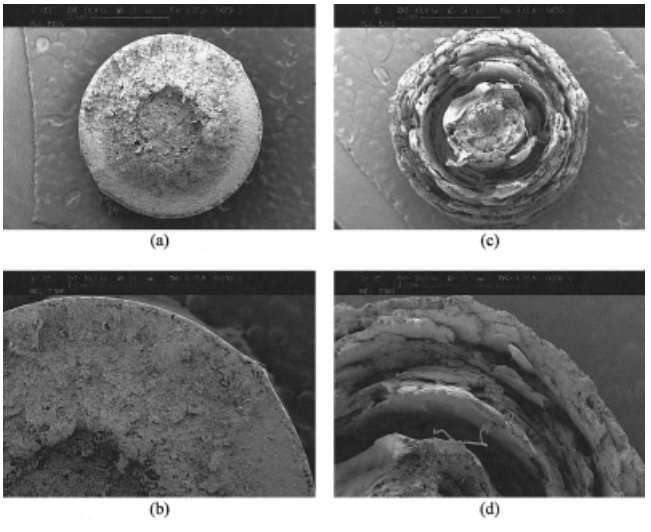

Figure 11 Scanning electron microscope (SEM) photographs of the tensile fracture surfaces of conventionally injection molded (a and b) and SCORIM-processed (c and d) HDPE/HAs composites.

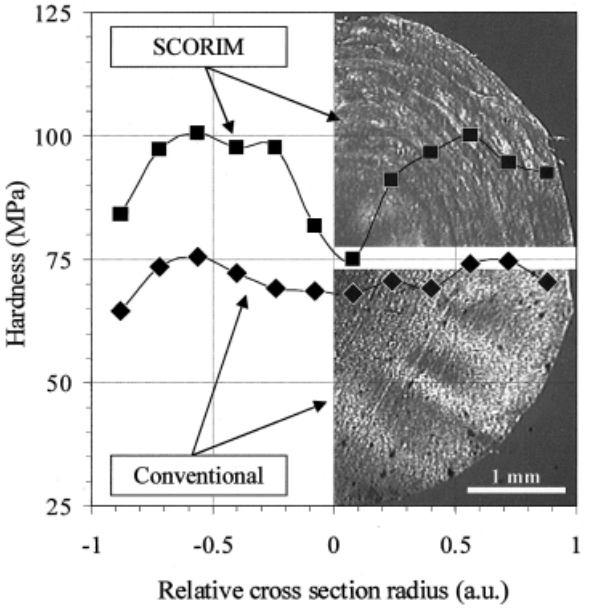

Figure 12 Microhardness variation along the cross section diameter for (♦) conventionally injection molded (CM) and (■) SCORIM-processed HDPE/HAs composites together with the respective polarized light microscope (PLM) photographs.

Shish-kebab structures featuring orientated fibrils and laterally grown stacked lamellae have been observed in elongational flow injection molded PE.[58] Although the thermomechanical environment associated with such a processing route[59] differs substantially from that encountered in SCORIM, the structural consequences are believed to be analogous for the two processes. Other molding techniques that also induce the shish-kebab formation and consequently lead to significant improvement of mechanical performance (in terms of stiffness and strength) are the high-pressure injection molding[60–62] and the oscillating packing injection molding;[63,64] this latter molding technique being a replica of the SCORIM process.

The microhardness variation along the diameter cross section for conventional and SCORIM HDPE/HAs moldings, together with the respective polarized light microscope (PLM) photographs, are plotted in Figure 12. The microhardness profile for conventionally molded HDPE/HAs specimens shows relative minima at both the vicinity of the mold wall and the core region. Conventionally molded HDPE and HDPE/HA specimens feature a skin region and a large spherulitic core.[65] Assuming that the contribu-

tion of the HA filler to the hardness is the same along the part diameter, the variations observed can be, in principle, attributed to dissimilarities within the polymer morphology. Baltá Calleja et al.[66] showed a correlation between hardness measurements and density in PE samples and inferred a similar correlation between hardness and crystallinity. For a temperature clearly above the glass transition temperature, the hardness of PE is directly proportional to the volume fraction and hardness of the crystalline phase. This hardness is influenced by the lamellae thickness of the deformed crystals.[66–69] For a given quotient between the basal surface free energy and the energy required for plastic deformation, the hardness of PE is inversely proportional to the reciprocal of the lamellae thickness. It is not possible to isolate the effect of either the crystallinity or the lamellae thickness on the quantified hardness variation along the part diameter. Nevertheless, the low value of hardness observed for conventional molding at the skin region is attributed to the high orientation but low crystallinity level of this rapidly cooled zone. Below this region, the small increase in hardness observed in the core direction derives from the high shear imposed on the melt in this region that dominates the crystallization process and promotes high crystallinity levels. As the distance from the mold wall further increases (towards the cross section centre), the effect of shear on the crystallization process diminishes and the crystallisation process is mostly determined by the cooling conditions (i.e., degree of undercooling).

The variation of microhardness for SCORIM processed samples is much more pronounced than that observed for the conventionally molded ones. An M-pattern profile, evident by observing Figure 12, defines three regions: a low crystallinity skin (in the vicinity of the frozen layer), a highly crystalline transition layer (associated with a clear laminated morphology), and a less crystalline core (central zone of the cross section). A study[70] on the structure and properties of a lower viscosity HDPE grade molded by SCORIM, combining microhardness measurements with differential scanning calorimetry experiments, also revealed the existence of such an M-pattern, attributing lower hardness and crystallinity values for both the skin and core regions. This result is in agreement with those from a study of Guan et al.[64] that showed the existence of higher crystallinity levels (inferred from calorimetric experiments) at intermediate distances from the mold wall and the core center as a result of a dominant-flow-induced crystallization process at this zone. The layered morphology observed in SCORIM-molded specimens features a highly crystalline anisotropic structure that sustains the mechanical performance improvement observed in the previous section. The delineation of the layered morphology on tensile testing arises from the structure discontinuity

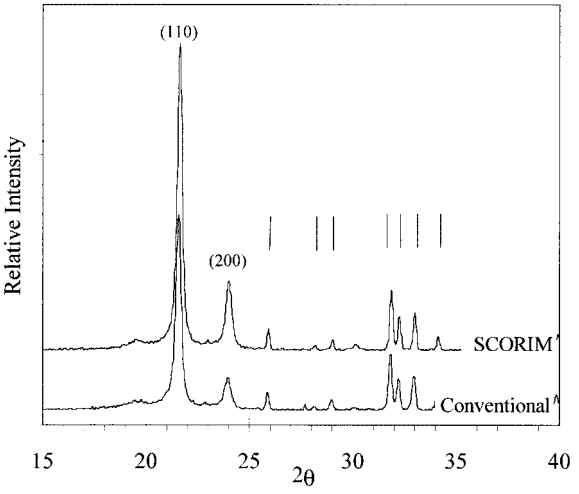

Figure 13 Wide-angle X-ray diffraction (WAXD) spectra for conventionally injection molded and SCORIM-processed HDPE/HAs composites.

of the SCORIM-processed specimens that alternate highly orientated layers, crystallized under the influence of shear, with thin spherulitic layers in between the former, crystallized during the interruptions of the shear flow between consecutive piston strokes.[71]

The higher overall crystallinity of the SCORIM processed composites as compared with conventional moldings is confirmed by the respective WAXD spectra for both cases presented in Figure 13. The higher crystallinity of the HDPE phase in SCORIM moldings as compared with those conventionally injection molded is confirmed by the more intense diffraction of the (110) and (200) crystallographic plans, which justifies the difference in microhardness observed between the two molding techniques. The anisotropy of the crystalline phase in HDPE/HA composites can be inferred from the WAXD patterns presented in Figure 14, which were obtained at discrete positions from the mold wall for both molding techniques. For all the patterns, the longitudinal direction of the tensile test bar [i.e., main direction of flow (MDF)] is parallel to the S–N direction in the figures. At the skin region (0.1 mm from the mold wall), the patterns for conventional and SCORIM moldings are very similar. At further distance (0.5 mm), it is possible to observe some arcing at the equatorial region of the Debye rings associated with the (110) and (200) reflections. This arcing becomes more pronounced as the distance from the mold wall further increases (1.5 mm), being more intense for the SCORIM moldings. This arcing reveals molecular orientation parallel to MDF as a consequence of the shear-induced crystallization process. At this distance (relative cross section radius of 0.6), the evident C-axis orientation of SCORIM moldings correlates well with the higher microhardness values measured at this zone. At the core region (2.5 mm),

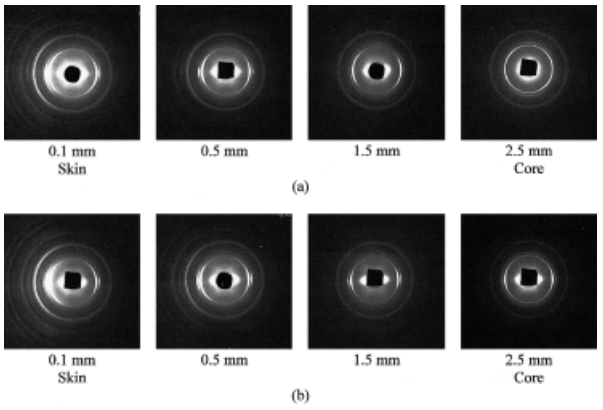

Figure 14 X-ray diffraction patterns taken along the cross-section diameter for (a) conventionally injection molded and (b) SCORIM-processed HDPE/HAs composites at positions of 0.1, 0.5, 1.5, and 2.5 mm from the mold wall.

conventional moldings are more isotropic, which constitutes further evidence of the higher orientation of the SCORIM-processed specimens. Additional X-ray patterns (not presented here) acquired for all the moldings at 1.5 mm from the mold wall exhibited signs of C-axis orientation for the SCORIM samples, which were never observed for those samples that were conventionally injection molded.

Morphology and interfacial interactions in HDPE/HA composites

The details of the tensile fracture surfaces of conventional (Figures 15a–15c) and SCORIM (Figures 15d–15f) moldings (already presented in Figure 11) are presented in Figure 15. At lower magnification (Figures 15a and 15d), the distinct deformation behavior of the matrices in the composites processed by the two methods is evident. Conventional moldings exhibit signs of considerable plastic deformation on tensile testing, whereas SCORIM moldings show, within each orientated layer, a more or less planar surface with reduced signs of deformation. At higher magnification (Figure 15b), it is possible to observe a fibrilar morphology developed in the HDPE matrix that is in agreement with its higher ductility. For both cases (Figures 15b and 15e), debonding of the HA particles occurs on tensile testing, which suggests a similar degree of interfacial interaction between the HDPE and the HAs particles for the two cases. The interfacial interaction in the composite appears to be limited to mechanical interlocking of the HA particles by the HDPE matrix (Figures 15c and 15f).

The use of coupling agents significantly enhances the ductility of the composites, as can be inferred the tensile fracture surface of conventionally injection molded HDPE/HAs + 0.5 wt % zirconate composite shown in Figure 16. An additional necking of the

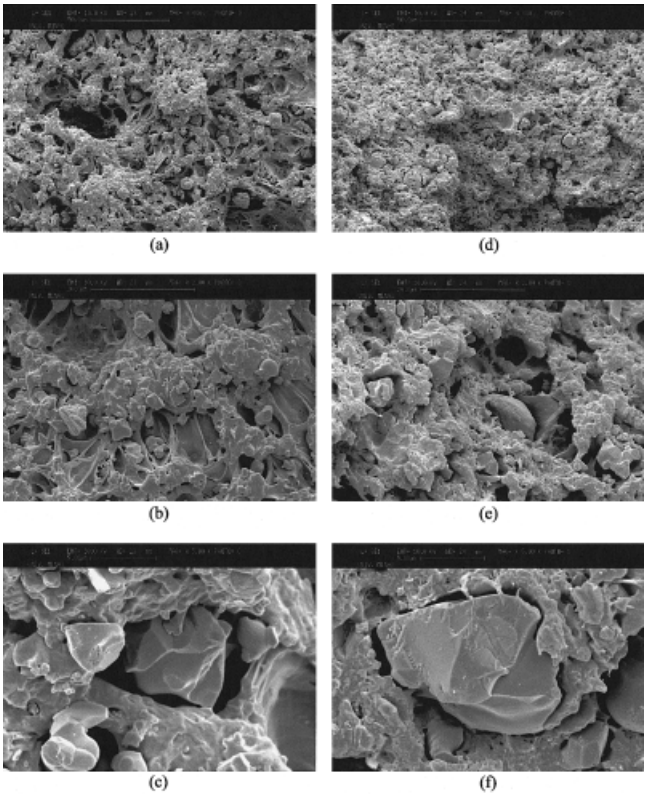

Figure 15 Scanning electron microscope (SEM) photographs showing details of the tensile fracture surfaces and of the polymer/ceramic interface for conventionally injection molded (a, b, and c) and SCORIM-processed (d, e, and f) HDPE/HAs composites.

tensile test bar, as compared with the uncoupled formulation (see Figure 11a), occurs during tensile testing (Figure 16a). The fracture surface (Figure 16b) shows signs of tearing and a great number of debonded particles and elongated voids.

The SEM photographs of the tensile fracture surfaces of conventionally injection molded HDPE/HAs composites and SCORIM-processed HDPE/HAs + 0.5 wt % titanate composites are shown in Figure 17. Conventionally molded HDPE/HAs composites exhibit a considerable number of a HA agglomerates (Figure 16a) with an average size ranging between 20

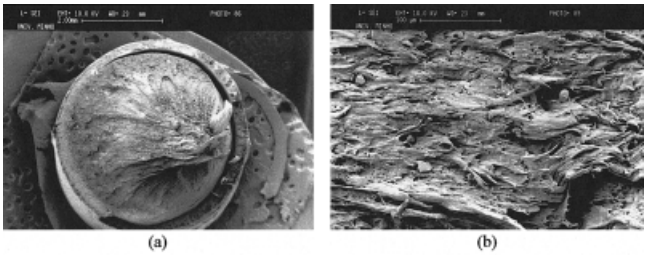

Figure 16 Scanning electron microscope (SEM) photographs of (a) general view and (b) respective detail of the tensile fracture surface of conventionally injection molded HDPE/HAs + 0.5 wt % zirconate composites.

and 80 μm. In this study, the term agglomerate refers to a collection of weakly bonded particles.[72] The application of shear during injection molding significantly reduces the number and size of such agglomerates. As previously shown, the reinforcement effect of the HA particles in the HDPE/HAs composites is enhanced by the application of shear (see first section), which is in agreement with the increase of HA dispersion reported here. Therefore, the enhancement in mechanical performance for HDPE/HA composites on the application of SCORIM can be attributed to both an increase in the matrix orientation and the filler dispersion. Further increase in filler dispersion is observed with the combined use of SCORIM and addition of coupling agents; compare Figure 17a with Figure 17b. The coupling agents act as dispersants of the HA filler in the composite.

It is proposed that titanium-based coupling agents react with surface protons at the surface of the filler, resulting in the formation of a monomolecular layer at the inorganic surface.[38] For the case of HA particles, this condensation is expected to occur due to the existence of available hydroxy groups present at the surface of the filler. It is evident that the effect of these agents strongly depends on the molding technique employed. Their reduced effect in conventional molding can be attributed to an uneven distribution of the agent as a result of insufficient mixing degree of the compound. It is believed that the incorporation of the coupling agent in the HDPE/HA mixture before extrusion is not adequate to achieve a homogeneous dispersion in the compound, resulting in zones with a shortage or excess of coupling agent. The excessive amount of coupling agent in discrete domains favors the condensation of a multilayer film at the surface of the particles, contributing to a decrease in stiffness. Furthermore, the uncondensed coupling agent will act as a plasticizer of the polymer matrix, which will further enhance the plasticizing effect of these additives.

The shear field applied during SCORIM application is believed to contribute to the disruption of the filler agglomerates and the dispersion of the coupling agent throughout the matrix. The SEM photographs of HA agglomerates in conventionally injection molded HDPE/HAs composites and SCORIM-processed HDPE/HAs + 0.5 wt % titanate composites are shown in Figure 18. The agglomerates observed in conventional molding (Figure 1 a) give place, in SCORIM moldings, to a scarce number of smaller agglomerates (Figure 18b) with an average size ranging between 5 and 30 μm. However, the HA particles in the coupled composites did not show any improvement in interfacial interaction towards the HDPE matrix compared with the uncoupled formulation. The existence of an eventual condensed layer at the surface of the HA particles did not improve its respective wetting by the polymer. This result is evidence of the dominant dispersant effect of the coupling agents on the composite system studied here.

The details of the tensile fracture surface of SCORIM-processed HDPE/HAns + 0.5 wt % titanate composites at both the skin (Figure 19a) and the core (Figure 19b) regions are shown in Figure 19. In both zones, the presence of HAns agglomerates is not evident. Conversely to the results for the HAs-based composites, all the HDPE/HAns composites (including the uncoupled formulation) exhibited a homogeneous distribution of the particles throughout the polymer matrix. It is believed that the even distribution of the particles assures the continuity of the polymer matrix and benefits the ductility of the composites. For this case, no significant improvement in filler dispersion or interfa-

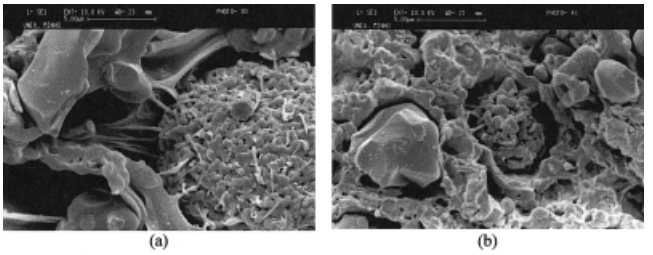

Figure 18 Scanning electron microscope (SEM) photographs of HA agglomerates in (a) conventionally injection molded HDPE/HAs composites and (b) SCORIM-processed HDPE/HAs + 0.5 wt % titanate composites.

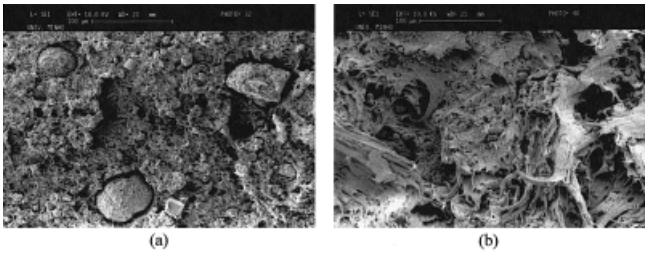

Figure 17 Scanning electron microscope (SEM) photographs of the tensile fracture surfaces of (a) conventionally injection molded HDPE/HAs composites and (b) SCORIM-processed HDPE/HAs + 0.5 wt % titanate composites.

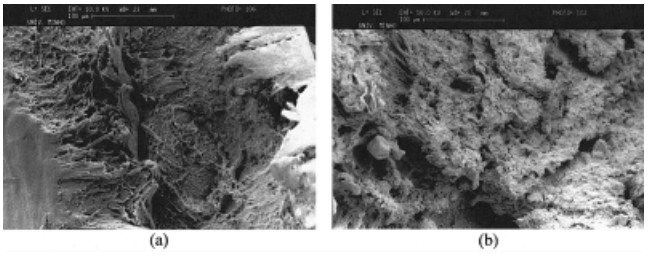

Figure 19 Scanning electron microscope (SEM) photographs of the tensile fracture surface of SCORIM processed HDPE/HAns + 0.5 wt % titanate composites in (a) the skin and (b) the core regions.

cial interaction was observed with the use of the coupling agents. This difference in behavior, as compared with the HDPE/HAs composites, can result from the smaller particle size and the higher surface area of the HAns filler that makes the coupling agent ineffective for the weight contents studied.

CONCLUSIONS

The incorporation of HA particles in HDPE improves stiffness and decreases tensile strength. The magnitude of the reinforcing effect depends on the molding technique used (conventional injection molding and SCORIM). The higher mechanical performance of the SCORIM-processed composites as proved by their high stiffness and tensile strength is the result of the strong anisotropic matrix and, to a lesser extent, the higher degree of filler dispersion. This high anisotropy is associated with a clear laminated morphology exhibiting high crystallinity and pronounced C-axis orientation as a result of a shear-induced crystallization process. The application of shear during injection molding also contributes to the disruption of the filler agglomerates.

The use of the titanate and the zirconate coupling agents caused significant variations in the tensile test behavior of the composites. However, their influence was very dependent on the molding technique employed. In conventional molding, these agents act mainly as plasticizers. The application of shear, by SCORIM, promotes the dispersion of the coupling agent, which further contributes to the disruption of the HA agglomerates. The combined use of coupling agents with shear application seems to be an effective route for the enhancement of the mechanical performance of HDPE/HA composites. However, the role of the titanate and zirconate additives as true coupling agents may be questionable. In this investigation no apparent improvement of the interaction between the filler and the matrix was observed. In spite of this result, an improvement in the mechanical performance of HDPE/HA composites is achieved as a result of the dominant dispersant effect. The difference in the reinforcing effect observed between HAs and HAns fillers arises from the lower particle size and higher final dispersion of the latter particles.

The research methodology followed has been shown to be a potential route for the development of bone-analogue composites with bone-matching mechanical performance. Maximum values of tensile modulus and strength of, respectively, 6.5 GPa and 90 MPa (in the bounds of human cortical bone) were obtained. Further improvements are expected from the selective replacement of HA particles by more efficient reinforcing systems (such as very stiff fibers like carbon fibers) and the use of other coupling systems.

The author (RAS) acknowledges the financial support by Subprograma Ciência e Tecnologia do 2° Quadro Comunitário de Apoio, Ministério da Ciência e Tecnologia (Portugal).

References

1. Fawcett, D. A Textbook of Histology; W.B. Saunders Company: Philadelphia, 1986.
2. Weiner, S.; Wagner, H.D. Ann Rev Mater Sci 1998, 28, 271.
3. Martin, R.B.; Burr, D.B. Structure, Function and Adaptation of Compact Bone; Raven: New York, 1989.
4. Ravaglioli, A.; Krawjewski, A.; Celloti, G.C.; Piancastelli, A.; Bachinni, B.; Montanari, L.; Zama, G.; Piombi, L. Biomaterials 1996, 17, 617.
5. Evans, G.P.; Behiri, J.C.; Bonfield, W.; Currey, J.D. J Mater Sci: Mater Med 1990, 1, 38.
6. Goldstein, S.A. J Biomech 1987, 20, 1055.
7. Carter, D.R.; Hayes, W.C. Clin Orthoped 1978, 135, 192.
8. Ziv, H.; Wagner, H.; Weiner, S. Bone 1996, 18, 417.
9. Weiner, S.; Arad, T.; Sabanay, I.; Traub, W. Bone 1997, 20, 509.
10. Bonfield, W. In Monitoring of Orthopaedic Implants; Burny, F., Pruers, R., Eds.; Elsevier Science: Amsterdam, 1993; p. 4.
11. Bonfield, W. J Biomech 1987, 20, 1071.
12. Keller, T.S.; Mao, Z.; Spengler, D.M. J Orthoped Res 1990, 8, 592.
13. Otani, T.; Whiteside, L.A.; White, S.E. J Biomed Mater Res 19993, 27, 575.
14. van der Sloten, J.; van der Perre, G.; Labey, L.; van Audekercke, R.; Helsen, J. J Mater Sci: Mater Med 1993, 4, 407.
15. Bonfield, W.; Grynpas, M.D.; Tully, A.E.; Bowman, J.; Abram, J. Biomaterials 1981, 2, 185.
16. Bonfield, W. J Biomed Eng 1988, 10, 522.
17. Huang, J.; Di Silvio, L.; Wang, M.; Tanner, K.E.; Bonfield, W. J Mater Sci: Mater Med 1997, 8, 775.
18. Huang, J.; Di Silvio, L.; Wang, M.; Rehman, I.; Ohtsuki, I.C.; Bonfield, W. J Mater Sci: Mater Med 1997, 8, 808.
19. Suwanprateeb, J.; Tanner, K.E.; Turner, S.; Bonfield, W. J Biomed Mater Res 1998, 39, 16.
20. Suwanprateeb, J.; Tanner, K.E.; Turner, S.; Bonfield, W. J Mater Sci: Mater Med 1997, 8, 469.
21. Wang, M.; Porter, D.; Bonfield, W. Br Ceram Trans 1994, 93, 91.
22. Guild, F.J.; Bonfield, W. Biomaterials 1993, 13, 985.
23. Tanner, K.E.; Downes, R.N.; Bonfield, W. Br Ceram Trans 1994, 93, 104.
24. Wang, M.; Ladizesky, N.H.; Tanner, K.E.; Ward, I.M.; Bonfield, W. J Mater Sci 2000, 35, 1023.
25. Ladizesky, N.H.; Ward, I.M.; Bonfield, W. Polym Adv Technol 1997, 8, 496.
26. Ward, I.M.; Bonfield, W.; Ladizesky, N.H. Polym Int 1997, 43, 333.
27. Ladizesky, N.H.; Ward, I.M.; Bonfield, W. J Appl Polym Sci 1997, 65, 1865.
28. Ladizesky, N.H.; Pirhonen, E.M.; Appleyard, D.B.; Ward, I.M.; Bonfield, W. Comp Sci. Technol 1998, 58, 419.
29. Deb, S.; Wang, M.; Tanner, K.E.; Bonfield, W. J Mater Sci: Mater Med 1996, 7, 191.
30. Wang, M.; Deb, S.; Tanner, K.E.; Bonfield, W. ECCM-7 1996, 2, 455–460.
31. Deb, S.; Wang, M.; Tanner, K.E.; Bonfield, W. In Proceedings of 12th European Conference on Biomaterials, Porto, Portugal, 10–13 September 1995.
32. Wang, M.; Deb, S.; Bonfield, W. Mat Letters 2000, 44, 119.
33. Reis, R.L.; Cunha, A.M.; Oliveira, M.J.; Campos, A.R.; Bevis, M.J. Mat Res Innovat 2001, 4, 263.
34. Kalay, G.; Sousa, R.A.; Reis, R.L.; Cunha, A.M.; Bevis, M.J. J Appl Polym Sci 1999, 73, 2473.

35. Wypych, G. Handbook of Fillers, 2nd Ed., ChemTec Publishing: New York, 1999.
36. Grossman, R.F. In Plastics Additives and Modifiers Handbook, 2nd ed.; Edenbaum, J., Ed.; Chapman & Hall: New York, 1996.
37. Rothon, R.N. In Particulate-Filled Polymer Composites; Rothon, R.N., Ed.; Longman Scientific & Technical: Harlow, U.K., 1995.
38. Monte, S.J. ; Sugerman, G. Polym Eng Sci 1984, 24, 18.
39. Iwashita, N.; Psomiadou, E.; Sawada, Y. Composites Part A 1998, 29A, 965.
40. Shiguo, D.; Jianfei, C.; Yinghong, X.; Faxiang, J.; Xiaoying, J. J Appl Polym Sci 1997, 63, 1259.
41. Arroyo, M.; Perez, F.; Vigo, J.P. J Appl Polym Sci 1986, 32, 5105.
42. Lee, N.J.; Jang, J. Composites Sci Technol 1997, 57, 1559.
43. Bajaj, P.; Jha, N.K. ; Jha, R.K. Polym Eng Sci 1989, 29, 8.
44. Liao, B.; Huang, Y.; Cong, G. J Appl Polym Sci 1997, 66, 1561.
45. Kharade, A.Y.; Kale, D.D. J Appl Polym Sci 1999, 72, 1321.
46. Xavier, S.F.; Schultz, J.M.; Friedrich, K. J Mater Sci 1990, 25, 2425.
47. Menon, N.; Blum, F.D.; Dharani, I.R. J Appl Polym Sci 1994, 54, 113.
48. Singh, B.;Verma, A.; Gupta, M. J Appl Polym Sci 1998, 70, 1847.
49. Hunt, K.N.; Evans, J.R.G.; Woodthorpe, J. Polym Eng Sci 1988, 28, 1572.
50. Hostalen Product Information, Germany.
51. Monte, S.J. Ken React Reference Manual Titanate, Zirconate and Aluminate Coupling Agents, Kenrich Petrochemicals, Inc., 1993.
52. Sim, C.P.; Cheang, P.; Liang, M.H.; Khor, K.A. J Mater Process Technol 1997, 69, 75.
53. Wang, M.; Joseph, R.; Bonfield, W. Biomaterials 1998, 19, 2357.
54. Xavier, S.F.; Schultz, J.M.; Friedrich, K. J Mater Sci 1990, 25, 2411.
55. Odell, J.A.; Grubb, D.T.; Keller, A. Polymer 1978, 19, 617.
56. Bashir, Z.; Odell, J.A.; Keller, A. J Mater Sci 1986, 21, 3993.
57. Bashir, Z.; Odell, J.A.; Keller, A. J Mater Sci 1984, 19, 3713.
58. Ania, F.; Baltá Calleja, F.J.; Bayer, R.K.; Tshmel, A.; Naumann, I.; Michler, G.H. J Mater Sci 1996, 31, 4199.
59. Bayer, R.K.; Zachman, H.G.; Baltá Calleja, F.J.; Umbach, H. Polym Eng Sci 1989, 29, 186.
60. Kubát, J.A.; Månson, J.A. Polym Eng Sci 1983, 23, 869.
61. Kubát, J.A.; Månson, J.A.; Rigdahl M. Polym Eng Sci 1983, 23, 877.
62. Boldizar, A.; Månson, J.A.; Rigdahl, M. J Appl Polym Sci 1990, 39, 63.
63. Guan, Q.; Shen, K.; Ji, J.; Zhu, J. J Appl Polym Sci 1995, 55, 1797.
64. Guan, Q.; Lai, F.S.; McCarthy, S.P.; Chiu, D.; Zhu, X.; Shen, K. Polymer 1997, 38, 5251.
65. Mano, J.F.; Sousa, R.A.; Reis, R.L.; Cunha, A.M.; Bevis, M.J. Polymer 2001, 42, 6187.
66. F.J. Baltá Calleja, Adv. Polym. Sci., 66 (1985)117.
67. Baltá Calleja, F.J. Trends Polym Sci 1994, 2, 419.
68. Flores, A.; Baltá Calleja, F.J.; Basset, D.C. J Polym Sci, Polym Phys Ed 1999, 37, 000.
69. Santa Cruz, C.; Baltá Calleja, F.J.; Asano, T.; Ward, I.M. Philos Magaz A 1993, 68, 209.
70. Sousa, R.A.; Reis, R.L.; Cunha, A.M.; Bevis, M.J., unpublished results.
71. Ogbonna, C.I.; Kakay, G.; Allan, P.S.; Bevis, J. J Appl Polym Sci 1995, 58, 2131.
72. Rothon, R.N.; Hancock, M. In Particulate-Filled Polymer Composites; Rothon, R.N., Ed., Longman Scientific & Technical: Harlow, U.K., 1995.